Journal of the Serbian Chemical Society
JSCS-info@shd.org.rs • www.shd.org.rs/JSCS
J. Serb. Chem. Soc. *89* (2) 215–230 (2024)
JSCS–5716
Original scientific paper
Published 2 March 2024

Physicochemical properties of bioplastic based on hydroxyethylcellulose and polyvinylpyrrolidone blend

BUDIMAN ANWAR*, CITRA NURHASHIVA, WAFA RAIHANAH ARWA and GALUH YULIANI

Material Chemistry Research Group, Chemistry Programs, Faculty of Mathematics and Natural Sciences Education, Universitas Pendidikan Indonesia, Jl. Dr. Setiabudhi 229, Bandung 40154, Indonesia

(Received 23 October, revised 7 November, accepted 25 December 2023)

Abstract: The aim of this study is to develop a bioplastic based on hydroxyethylcellulose (HEC) and polyvinilpyrrolidone (PVP) which is applied as packaging materials. The effect of incorporation of PVP into HEC on the physicochemical properties of its blend films are investigated. The FTIR and DSC analysis denote that incorporation of PVP induce the intermolecular hydrogen bonds to occur more intensely. The XRD diffractograms indicate that the incorporation of PVP reduces the crystallinity of the film. The mechanical properties of the films become greater as the PVP content increases, and the optimum composition of HEC/PVP is at 5:3 mass ratio with a tensile strength of 34.8±3.4 MPa; elongation at break 104.3±4.9 %; and an elastic modulus of 0.10±0.02 GPa. The SEM and DSC analysis signify an excellent compatibility and miscibility between HEC and PVP. The incorporation of PVP increase the transparency and hydrophilicity of the film. The water vapor transmission rate of the films is relatively unchanged due to the incorporation of PVP. The TGA and DSC analysis reveal that the incorporation of PVP increases the thermal stability and the glass transition temperature of the film. This bioplastic film could be an alternative for biodegradable packaging material.

Keywords: polyblend; biodegradable plastic; cellulose derivative; biopolymers; HEC/PVP blend.

INTRODUCTION

Plastic as petrochemical-based synthetic polymers is one of the most produced, used and versatile materials due to its excellent flexibility, durability and resistance. Nevertheless, exaggerated use of durable plastics, mainly for packaging materials, have made them a big problem because of their build-up in the environment are greater than their degradation rate in landfills.[1,2] Nowadays,

* Corresponding author. E-mail: budimananwar@upi.edu
https://doi.org/10.2298/JSC231023103A

there is an augmentative interest in bio-based plastics. The use of biopolymers as a substitute to petrochemical-based synthetic polymers for packaging materials has increased due to their availability, sustainabilty, non-toxicity, relatively low cost, biocompatibility and biodegradability.[3] Several biopolymers have been utilized for plastic packaging films such as carrageenan,[4] pectin,[5] alginate,[6] starch[2] and various cellulose derivatives.[7,8]

Physical blending of polymers is one of the most convinient method to modify polymeric materials to obtaine new materials with the desired properties. In order to meet the need for new materials, physical blending could regularly be performed more swiftly and economically than synthesizing materials with novel molecules. Physical blending between biopolymers and synthetic polymers deputize a new class of materials and have gained much attention particularly in bioapplications and as biodegradable packaging materials.[7]

Hydroxyethyl cellulose (HEC) is a nonionic water-soluble cellulose ether and one of the most significant cellulose derivatives (cellulose ether). HEC is obtained by treating cellulose with sodium hydroxide and reacting with ethylene oxide.[9] HEC has very wide applications, including in cosmetics, pharmaceutical, paint industry and battery.[10] This is because HEC has low toxicity, non-immunogenicity and biocompatibility.[11] Moreover, HEC has good film forming and biodegradability properties.[9]

Polyvinilpyrrolidone (PVP) is synthesized by free radical polymerization from *N*-vinylpyrrolidone monomer with AIBN as the initiator.[12] PVP is a high molecular amorphous polymer that dissolve easily in water and several organic solvents, and also has excellent thermal properties. Addtionally, PVP has good biocompatibility, is good complexing agent and non-toxic.[13]

Previous studies have reported on miscibility of HEC with several synthetic polymers, including polyethylenglycol (PEG),[14] polyvinylalcohol (PVA)[15] and PVP.[16] In this study, we have examined the effect of incorporation of PVP into HEC on the physicochemical properties of blend films. The polyblend films were prepared by solution casting method with different composition of HEC and PVP with the addition of a certain amount of glycerol as a plasticizer. The mechanical, morphological, optical, thermal, and moisture barrier properties of the blend films were thoroughly characterized.

EXPERIMENTAL

Materials

HEC technical grade, PVP K30, and glycerol technical grade were purchased from Interco Laboratories, Bandung, Indonesia. All other reagents were of analytical grade and commercially available.

Preparation of blend films

The HEC/PVP blend films were prepared by solution casting method. To obtain an HEC/ /PVP blend film with a composition of 5:3 mass ratio, 1.25 g of HEC was dissolved in 30 mL

of distilled water and stirred rigorously for 10 min at room temperature. A certain amount of glycerol was added to the HEC solution so that the glycerol composition in film blend was 5 %, and stirring continued for 10 min. Then, 0.75 g of PVP was dissolved in 20 mL of distilled water and stirred rigorously for 10 min at room temperature. Subsequently, both solutions were mixed together and stirred continuosly for 20 min to ensure the homogeneous of the solutions in the blend. The mixture was then degassed ultrasonically for 2 min. Afterwards, casting was undertaken by pouring the mixture into a number of petridishes and then allowed to dry. When dried the films were peeled out of the petridishes and stored in desiccators to prevent moisture. The same procedure was performed for other compositions, *i.e.*, 6:2, 7:1 and 8:0.

Characterization

Mechanical properties including tensile strength, elongation at break, and Young's modulus were characterized using the Textechno Favigraph I-PI-067 instrument at a crosshead speed of 6.0 mm/min under dry conditions at room temperature. All films were cut using the same shaper. The size of the test samples was 3 mm in width and 50 mm in parallel length.

Fourier-transform infrared (FTIR) spectroscopy was carried on FTIR-600 (Jaco Corp, Japan) instrument. The samples analyzed in the frequency range of 4000–400 cm^{-1} with scanning resolution of 2 cm^{-1} to find the information about the changes in chemical composition and crystallinity. Crystallinity ratio (*CrR*) of cellulose and its derivative could be acquired by comparing the absorbance peaks at 1372 (A_{1372}) and 2900 cm^{-1} (A_{2900}):[17,18]

$$CrR = A_{1372} / A_{2900} \tag{1}$$

The hydrogen bond energy (E_H) for several OH stretching bands is calculated as follows:[17]

$$E_H = \frac{v_0 - v}{kv_0} \tag{2}$$

where v_0 is the standard frequency corresponding to free OH groups (3650 cm^{-1}), v is the frequency of the bonded OH, and k is a constant ($1/k = 2.625\times10^2$ kJ/mol). Whilst, the hydrogen bond distance (R) is obtained as follows:[17]

$$\Delta v\ (cm^{-1}) = 4430(2.84 - R) \tag{3}$$

where $\Delta v = v_0 - v$, v_0 is the frequency of monomeric OH stretching (3600 cm^{-1}), and v is the stretching frequency observed in the infrared spectra of the cellulose samples.

The XRD analysis is conducted to investigate the crystallinity index (*CI*) and crystallite size (L) of the film samples. The diffractograms of HEC and HEC/PVP blend films are obtained at room temperature by MiniFlex (Rigaku, Japan) X-ray diffraction instrument using CuKα radiation (λ = 1.54 Å) in the 2θ range of 3–90°. Potential difference and current used are 40 kV and 15 mA, consecutively. The XRD analysis is conducted to investigate the *CI* and L. The crystallinity index of the films can be estimated from the ratio of the crystalline peak area to total and calculated using as follows:

$$CI = 100\frac{\text{Area of crystalline phase}}{\text{Area under the all peaks}} \tag{4}$$

The crystallite size is calculated using the Scherrer equation:

$$L = \frac{K\lambda}{H\cos\theta} \tag{5}$$

where K is a constant that Scherrer found to e 0.94; λ is the X-ray wavelength (0.154 nm); H is the full width at half maximum (FWHM) in rad and θ is the Bragg angle.[17]

In order to examine the morphology of films and miscibility of HEC and PVP in blend, the film specimens were coated by gold/palladium using ion sputter coater and observed by EVO MA 10 scanning electron microscope (SEM, Carl Zeiss, Germany) with the operated voltage at 15 kV.

The light transmission and opacity of films were determined using a UVmini-1240 UV––Vis spectrophotometer (Shimadzu, Japan). The light transmission was measured at a wavelength of 200–600 nm with air as a blank.[19] Opacity of the films was calculated as follows:

$$\text{Opacity} = \frac{\text{Absorbance at 600 nm}}{\text{Film thickness (mm)}} \tag{6}$$

A set of laboratory-scale experimental tools were used to measure the water contact angles on film surfaces. Film specimen measuring 10 mm×10 mm was mounted on a platform, onto which distilled water was dropped from a syringe. The water droplet on the surface of film was captured by the camera. The images were then processed using the ImageJ software to acquire the contact angle data, that were used to evaluate the hydrophobicity of films.

The water vapor transmission rate (*WVTR*) was conducted using a method adapted from preceding report with some modifications.[20] The film specimens made into a vial lid which had been filled with 50 g of silica gel until all parts of the vial were covered. Moreover, the vial was put into desiccator which had previously been filled with 120 mL of distilled water instead of silica gel. The silica gel was then weighed after 24 h. *WVTR* was calculated as follows:

$$WVTR = \frac{\Delta W}{At} \tag{7}$$

where ΔW is the change in mass of silica gel after 24 h (g), A is film surface area (mm), and t is time (24 h).

The glass transition temperature (T_g) and the chang in enthalpy of relaxation (ΔH_{relax}) of films were investigated by differential scanning calorimetry (DSC) using DSC-214 Polyma (Netzsch, Germany) under nitrogen atmosphere. Film specimens were sealed hermetically in DSC pans and heated from 25 to 250 °C at a rate of 10 °C/min.

Thermogravimetric analysis (TGA) was performed by TGA701 thermogravimetric analyzer (Leco, USA) to determine the thermal stability of films. The certain mass of each film specimen was sealed hermetically in TGA pans and heated from 25 to 600 °C with heating rate of 5 °C min^{-1} under nitrogen atmosphere. The thermal decomposition temperature (T_d) and derivative thermogravimetric curve (DTG) were obtained.

RESULTS AND DISCUSSION

Optimization and mechanical properties of blend films

Fig. 1 shows the photographs of blend films with different composition of HEC and PVP. It can be seen that all films are transparent.

Mechanical properties play an important role in packaging area. Considering that fact, in this study the mechanical properties were applied as optimization parameters. Table I represents the mechanical properties of the blend films. The optimum composition of HEC/PVP blend film is at 5:3 mass ratio since it has

mechanical properties comparable to LDPE, *i.e.*, tensile strength 8–31 MPa, elongation at break 100–965 %, and Young's modulus 0,2–0,5 Gpa.

(a) (b) (c) (d)

Fig. 1. Photographs of: a) HEC; b) HEC/PVP (7:1); c) HEC/PVP (6:1); d) HEC/PVP (5:3) films.

TABLE I. Mechanical properties of HEC and HEC/PVP blend films

Sample	Tensile strength, MPa	Elongation at break, %	Young's modulus, GPa
HEC	11.1±3.6	96.9±5.6	0.072±0.01
HEC/PVP (7:1)	10.6±3.0	81.0±9.7	0.067±0.01
HEC/PVP (6:2)	18.5±2.9	82.4±7.7	0.073±0.02
HEC/PVP (5:3)	34.8±3.4	104.3±4.9	0.105±0.03

The mechanical properties of the blend are mostly determined by molecular interactions that occur in the blends. HEC has many hydroxyl groups as proton donors. Whereas, PVP could act as a proton acceptor since it has a carbonyl group on its pyrrolidone ring. As a result, hydrogen bond interactions will ensue between the two polymers.[21] The molecular mass of the polymer, concentration, process of blending, and solvent evaporation may also influence the mechanical properties of the films.[22]

As shown in Table I, the tensile strength, elongation at break, and Young's modulus all become greater as the PVP composition increases. The increase in tensile strength and Young's modulus could be linked to the intermolecular hydrogen bonds and other secondary intermolecular forces that occur more intensely as increasing PVP content.[23,24] This occurrence was evidenced by FTIR and DSC analysis. Whilst, the increase in elongation at break could be attributed to the crystallinity that decrease as increasing PVP content. For semi-crystalline polymers, the amorphous phases can deform more freely.[25] This occurrence also was evidenced by FTIR and XRD analysis.

FTIR analysis

Fig. 2 shows the FTIR spectra of HEC, PVP and blend films with different composition of HEC/PVP. The FTIR spectrum of HEC provides the characteristic absorption bands at 3429, 2924, 1383, 1122 and 1062 cm^{-1}; these bands are assigned to O–H stretching, C–H stretching, CH_3 asymmetric bending, C–O–C

asymmetric stretching and C–O stretching, respectively.[26] Whilst, the characteristic absorption bands at 2955, 1659, 1433 and 1287 cm^{-1} in FTIR spectrum of PVP are attributed to the stretching vibrations of C–H, C=O, C=C and C–N, respectively. The broad band at 3427 cm^{-1} indicates that PVP contains absorbed water.[27]

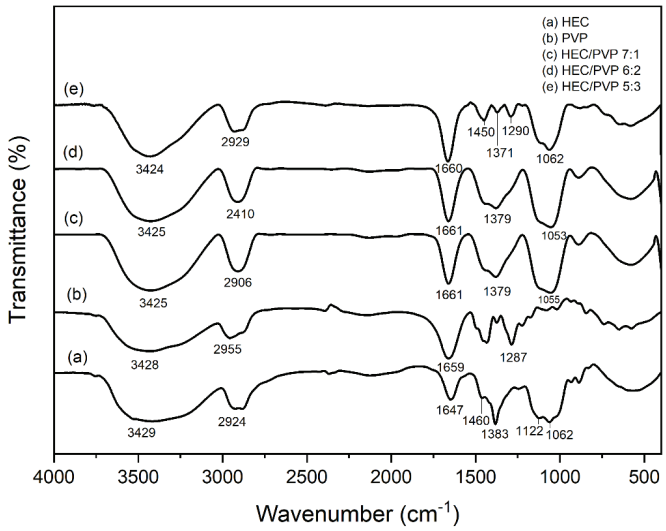

Fig. 2. FTIR spectra for HEC, PVP and HEC/PVP blend films.

The characteristic bands of HEC and PVP appeared in the spectra of HEC/ /PVP blend films. Nevertheless, there is a shift in the absorption band of O–H in HEC to the lower frequency. This is due to the formation of hydrogen bonds between HEC and PVP in the blend films.[28] The values of hydrogen bonds energy (E_H) and hydrogen bond distances (R) for HEC and HEC/PVP blend films were obtained using Eqs. (2) and (3), respectively, and presented in Table II. The value of E_H become greater as the PVP composition increases, and *vice versa* for the R value. Both parameters evidence that intermolecular hydrogen bonds occur more intensely as the PVP content increases.[21] These results confirm mechanical properties, mainly the tensile strength and Young's modulus of films.

TABLE II. The value of crystallinity ratio (CrR), hydrogen bond energy (E_H), and hydrogen bond distance (R) for the HEC and blend films

Sample	*CrR*	E_H / kJ mol^{-1}	R / Å
HEC	1.41	15.89	2.8014
HEC/PVP (7:1)	1.19	16.18	2.8005
HEC/PVP (6:2)	1.23	16.18	2.8005
HEC/PVP (5:3)	0.25	16.25	2.8003

The crystallinity ratio (*CrR*) of HEC and HEC/PVP blend films acquired by Eq. (1) are presented in Table II. The decreasing *CrR* value as the PVP content increases indicates that the crystallinity of the blend films decrease as the PVP content increases. This is due to the PVP molecules that prevent HEC molecules to re-organize during film formation. In addition, the absorption peak at about 1650 cm^{-1} in HEC spectrum is related to water which is absorbed in the amorphous region.[26] As seen in Fig. 2, the absorption band intensity at around 1650 cm^{-1} in the HEC/PVP blend films are greater than that of HEC. This also signifies that the HEC/PVP blend films have lower crystallinity than HEC film.

XRD analysis

The X-ray diffraction patterns of HEC and HEC/PVP blend films are displayed in Fig. 3.

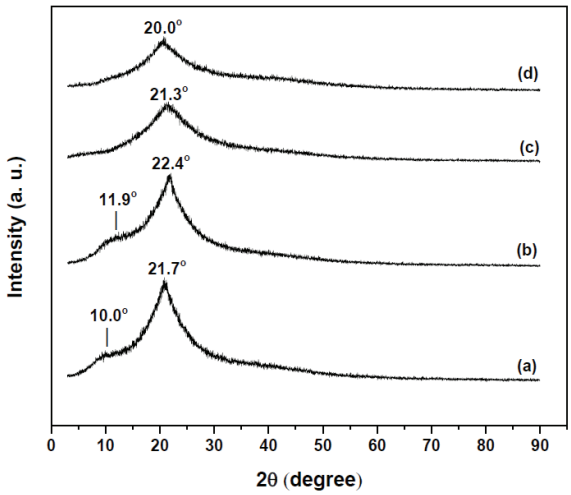

Fig. 3. X-ray diffraction pattern of: a) HEC, b) HEC/PVP (7:1), c) HEC/PVP (6:2) and d) HEC/PVP (5:3) films.

As shown in Fig. 3, the HEC film provide the diffraction peaks at about 2θ 10.0 and 21.7° which are typical to the structure of crystalline HEC.[29] After the incorporation of PVP into HEC (Fig. 3, curves b–d), the broadening of the peaks was observed with lower intensity. Moreover, the diffraction peak at about 2θ 10.0° disappeared in the XRD patterns of HEC/PVP with higher PVP content (Fig 3, curves c and d). The crystallinity index value decreases as the PVP content increases (Table III). This can be related to decrease in crystallinity due to restricted segmental movement by the incorporated PVP in the HEC.[30] Moreover, the incorporation of PVP into HEC would destroy the original semi-crystalline structure of HEC by leading to an amorphous structure.[29] This finding is in

accordance with the FTIR analysis and in turn can clarify the mechanical properties, mainly the elongation at break.

TABLE III. The value of crystallinity index (CI) and crystallite size (L) for the HEC and blend films

Sample	2θ / °	*FWHM*[a] / °	*d*-spacing, nm	*CI*[b] / %	L[c] / nm
HEC	21.70	5.45	0.41	40.86	9.58
HEC/PVP (7:1)	22.42	5.12	0.40	37.02	10.20
HEC/PVP (6:2)	21.35	9.39	0.42	27.82	5.56
HEC/PVP (5:3)	20.02	6.40	0.44	24.68	8.16

[a]The full width at half maximum of XRD profiles; [b]calculated using Eq. (4); [c]calculated using Eq. (5)

The crystallite size (L) values of both HEC film and HEC/PVP blend films are shown in Table III. The crystallite size values show some variation despite of showing constant affect, by the incorporation of the PVP content. However, with higher content of PVP, the crystallite size decrease, which may be associated to variation in cooling rate or annealing process.[30] French and Cintron[31] suggest that there is a nonlinear relationship of crystallinity index to the relative crystallite size for a given structure. Hence, the crystallinity index may not purely relate to the crystallite size.

SEM analysis

Fig. 4 shows the surface morphologies of films detected by SEM. Both the HEC and HEC/PVP films have homogeneous surface. This confirms the compatibility and miscibility of both polymers.[22] Moreover, the HEC/PVP blend film has more delicate surface than HEC film. This can be comprehended since PVP plays a role as a good film-forming agent. The compatibility and miscibility of the two polymers was further evidenced by DSC analysis.

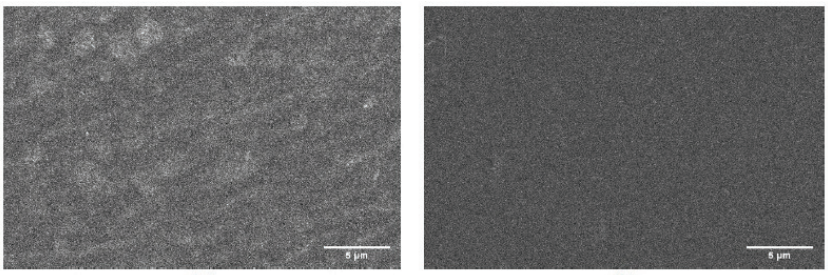

(a) (b)

Fig. 4. SEM image for (a) HEC film and (b) HEC/PVP 5:3 blend film.

Optical properties

One of the important factors that should be examined in the manufacture of plastic packaging are optical properties.[32] The most considerably used method to

investigate the optical properties of a film is determining the opacity value of the film. Opacity is defined as the ratio between the absorbance at 600 nm and the film thickness. The opacity values of HEC film (Fig. 1a) and HEC/PVP 5:3 blend film (Fig. 1d) which was obtained using equation (4) are presented in Table IV.

TABLE IV. The opacity value of the HEC and HEC/PVP 5:3 blend films

Sample	Thickness, mm	Absorbance at 600 nm	Opacity, A/mm
HEC	0.144	0.217	1.509
HEC/PVP 5:3	0.228	0.296	1.300

The opacity value is conversely related to the transparency. An increase in the opacity value signifies a decrease in transparency.[33] The opacity value is strongly influenced by the internal structure and surface characteristics. Amorphous polymers have lower opacity values (more transparent) than crystalline one. When molecules with a crystalline arrangement increase, a different refractive index is formed from each part of the crystalline structure, which in turn increases the opacity value (less transparent).[34] The opacity value of films presented in Table IV indicate that the incorporation of PVP into HEC increases the transparency of the film. The results of the optical properties analysis are in accordance with the results of the FTIR and XRD analysis.

Contact angle measurement

Measuring the contact angle of water drop on the surface of a film can be used to determine the hydrophilicity of a film.[35] The value of the contact angle < 90° signifies that the film is hydrophylic. This value also indicates that the film has a high surface energy, so water will wet the surface properly. Contrarily, if the surface energy of the film is low, so water does not wet the surface well. In this case, the value of the contact angle will increase and the film is categorized as hydrophobic.[36]

The contact angle of HEC film and HEC/PVP 5:3 blend film are shown in Fig. 5. It reveals that the contact angle of HEC and HEC/PVP 5:3 blend films are 66.38 and 54.36°, successively. The decline in contact angle is affected by the hydrophilic properties of PVP which contains hydrophilic groups in its molecules.[37] This result deduces that the incorporation of PVP into HEC increases the film hydrophilicity.

Water vapor transmission rate

Water vapor transmission rate (*WVTR*) is one of an important feature in establishing the barrier properties of plastic packaging. The *WVTR* value of the film indicates the quantity of moisture that has passed through the film. Therefore, the value of *WVTR* depicts a film's resistance towards water vapor transmission under particular conditions. The frequently plastic films used as packaging

have relatively slight *WVTR* value (approximately 5–20 g/m^2 h) which refers to good barrier properties.[38,39]

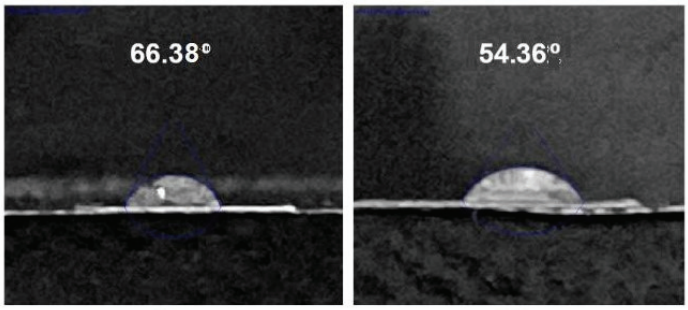

Fig. 5. Contact angle of (a) HEC film and (b) HEC/PVP 5:3 blend film.

The value of *WVTR* is strongly relate to hydrophilicity and porosity of the film-forming materials.[40] The values of *WVTR* for HEC film and HEC/PVP 5:3 blend film acquired, using Eq. (5) successively, are 91.91 and 91.93 g/m^2 h. These values are categorized as medium barrier properties. Hence, the addition of PVP into HEC relatively does not change the barrier properties of the film against water vapor.

DSC analysis

The effect of incorporation of PVP into HEC on T_g and ΔH_{relax} was investigated by DSC technique. There are three types of glass transition temperatures (T_g), *i.e.*, the primary (α) transition, β-transition and γ-transition. The primary transition transpires in the amorphous regions of the polymer. The secondary transition called the β-transition correlates with the mobility of side groups or smaller unit backbone chains. Another secondary transition designated the γ-transition is related to the end-group rotation, crystalline defects, backbone-chain motions of short segments or groups and phase separation of impurities or diluents. The β-transition is higher than the γ-transition.[41] Generally, the primary transition for HEC vary from 90 to 120 °C,[42,43] the β-transition between 0 and 40 °C[41] and the γ-transition among −60 and −120 °C.[41]

The DSC thermograms for HEC and HEC/PVP 5:3 blend films are shown in Fig. 6. The DSC thermograms of HEC and HEC/PVP 5:3 blend films denoted a relatively wide endotherms glass transition temperature (T_g) successively at 90.9 and 92.5 °C. These relatively broadened glass transitions corresponded to a primary transition that occurs in amorphous region of semi-crystalline materials. ΔH_{relax} for HEC and HEC/PVP 5:3 blend films were 255.3 and 310.2 J/g, respectively. These results designate that the intermolecular hydrogen bonds and other secondary intermolecular forces take place more intensely in HEC/PVP 5:3

blend instead in HEC. More vigorous hydrogen bonds and other secondary intermolecular forces will induce the mobility of side groups or smaller unit backbone chains to be obstructed, leading to high T_g and ΔH_{relax}.[42,44] This finding is in accordance with the FTIR analysis and confirms the mechanical properties, *i.e.*, tensile strength and Young's modulus.

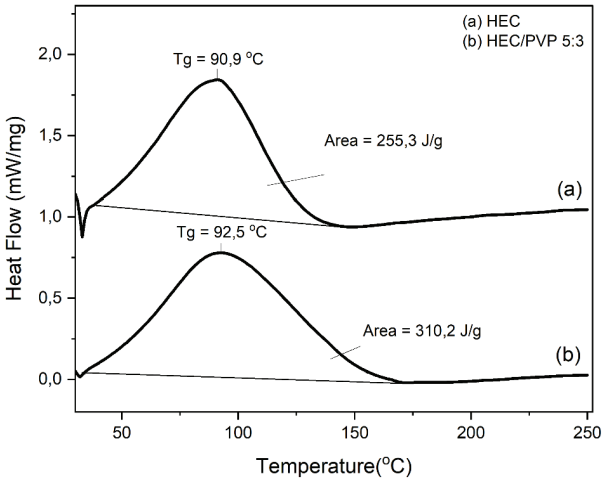

Fig. 6. DSC thermograms of: a) HEC film and b) HEC/PVP 5:3 blend film.

It was observed that in DSC thermogram of HEC/PVP film showed only single broad curve of T_g. This result attribute to the compatibility and miscibility of HEC and PVP.[42] The finding is also in accordance with the SEM analysis.

Thermogravimetric analysis

The other thermal properties of the HEC and HEC/PVP 5:3 blend films were examined by the TGA technique to investigate the thermal stability, composition and thermal degradation kinetics of films. Fig. 7a shows the TGA curves for HEC and HEC/PVP 5:3 blend films which characterized the thermal destruction of all films in nitrogen atmosphere. The derivative thermogravimetric (DTG) curves in Fig. 7b show the temperature of the starting point of decomposition (T_0) and the maximum speed of the thermal degradation (T_{max}) of films.

From the TGA curves, the heating from 27 to 150 °C the weight of HEC film is decreased about 14 %, whilst the HEC/PVP 5:3 blend film is about 16 %. This initial weight loss is due to moisture evaporation or weakly bound water.[26,44] This is also might be due to splitting or volatilization of small molecules from the samples.[42] On following heating runs, the further weight loss was observed both in the HEC and HEC/PVP 5:3 blend films. The starting point (T_0) of the second stage decomposition of the HEC film was observed at about 273 °C with the maximum rate (T_{max}) at about 314 °C, which attribute to the cellulose ethers

degradation including the parallel processes of dehydration and demethoxylation.[45] Whereas, the second stage of the HEC/PVP 5:3 blend film decomposition started (T_0) at about 284 °C with T_{max} at about 334 °C, both of which were higher than those HEC film. This indicates that HEC/ PVP 5:3 blend film has more excellent thermal stability than HEC film. Hereafter, the third stage of the HEC/PVP 5:3 blend film decomposition was observed at about 370 °C (T_0) with T_{max} at about 406 °C which appertain to the degradation of PVP.[46] The thermal degradation properties of the HEC and HEC/PVP 5:3 blend films are summarized in Table V.

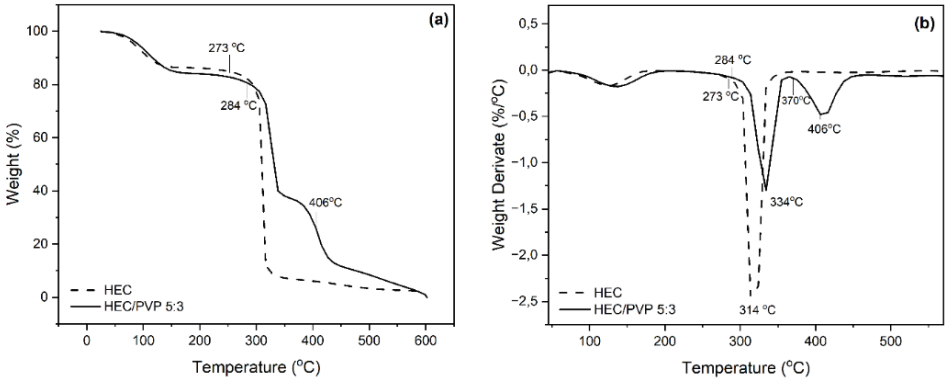

Fig 7. a) TGA and b) DTG curves for the HEC and HEC/PVP 5:3 blend films.

TABLE V. Thermal degradation properties of the HEC and HEC/PVP 5:3 blend films

Sample	Initial stage			Second stage			Third stage			
	T_0 °C	T_{max} °C	*WL* %	T_0 °C	T_{max} °C	*WL* %	T_0 °C	T_{max} °C	*WL* %	Char yield
HEC	50	125	14	273	314	78	–	–	–	8
HEC/PVP 5:3	50	140	16	284	334	48	370	406	24	12

CONCLUSION

The present study is focused on the investigation of physicochemical properties of HEC and HEC/PVP blend films. All films are prepared by solution casting methods with the addition of 5 % of glycerol as a plasticizer. The mechanical properties of blend films increase with increasing PVP content. The optimum composition of HEC/PVP blend is at 5:3 mass ratio with mechanical properties comparable to LDPE (tensile strength of 34.8±3.4 MPa; elongation at break 104.3±4.9 %, and an elastic modulus of 0.105±0.03 GPa). The surface morphology of the HEC/PVP 5:3 blend film more delicate and homogeneous than those of the HEC film, suggesting a good miscibility between HEC and PVP. The incorporation of PVP into HEC reduces the crystallinity of the film,

but on the other hand it causes hydrogen bonds and other secondary forces to occur more intensely. The HEC/PVP 5:3 blend film (opacity = 1.300 A/mm; contact angle = 54.36°) is more transparent and hydrophilic than HEC film (opacity = 1.509 A/mm; contact angle = 56.40°). The barrier properties of HEC (*WVTR* = 91.91 g/m^2 h) and HEC/PVP 5:3 blend (*WVTR* = 91.93 g/m^2 h) films are almost no different, and both have moderate barrier properties. The HEC/ /PVP 5:3 blend film has a good thermal stability up to 284 °C. The excellent polyblend film from low cost and environmentally friendly source could be an alternative for biodegradable packaging material.

Acknowledgement. This work was supported by the Research and Community Service Grants, Universitas Pendidikan Indonesia Funds in 2023, Competency Strengthening Research Scheme.

ИЗВОД

ФИЗИЧКО–ХЕМИЈСКА СВОЈСТВА БИОПЛАСТИКЕ НА БАЗИ СМЕШЕ ХИДРОКСИЕТИЛЦЕЛУЛОЗЕ И ПОЛИ(ВИНИЛ-ПИРОЛИДОНА)

BUDIMAN ANWAR*, CITRA NURHASHIVA, WAFA RAIHANAH ARWA и GALUH YULIANI

Material Chemistry Research Group, Chemistry Programs, Faculty of Mathematics and Natural Sciences Education, Universitas Pendidikan Indonesia, Jl. Dr. Setiabudhi 229, Bandung 40154, Indonesia

Циљ ове студије је развој биопластике засноване на хидроксиетилцелулози (HEC) и поли(винил-пирилидона) (PVP) који се примењује као материјал за паковање. Истраживан је ефекат уношења PVP u HEC на физичко–хемијска својства филмова бленди. FTIR и DSC показују се да се увођењем PVP интензивније стварају међумолекуларне водоничне везе. XRD дифрактограми указују на то да уградњом PVP смањује кристаличност филма. Механичка својства филмова постају боља како се PVP масени садржај повећава, а оптимални састав HEC/PVP је на 5:3 са јачином на кидање од 34,8±3,4 MPa; издужење при кидању 104,3±4,9 %; и модул еластичности од 0,10±0,02 GPa. SEM и DSC анализа показују одличну компатибилност и мешљивост између HEC и PVP. Укључивање PVP повећава транспарентност и хидрофилност филма. Брзина преноса водене паре филмова остаје релативно непромењена уградњом PVP. TGA и DSC показују да уношење PVP повећава топлотну стабилност и температуру стакластог прелаза филма. Овај биопластични филм могао би да буде алтернатива за биоразградиви материјал за паковање.

(Примљено 23. октобра, ревидирано 7. новембра, прихваћено 25. децембра 2023)

REFERENCES

1. S. Jeremic, J. Milovanovic, M. Mojicevic, S. S. Bogojevic, J. Nikodinovic-Runic, *J. Serb. Chem. Soc.* **85** (2020) 1507 (https://doi.org/10.2298/JSC200720051J)
2. K. E. Rivadeneira-Velasco, C. A. Utreras-Silva, A. Díaz-Barrios, A. E. Sommer-Márquez, J. P. Tafur, R. M. Michell, *Polymers* **13** (2021) 3227 (https://doi.org/10.3390/polym13193227)
3. G. El-Fawal, H. Hong, X. Song, J. Wu, M. Sun, C. He, X. Mo, Y. Jiang, H. Wang, *Food Packag. Shelf Life* **23** (2020) 100462 (https://doi.org/10.1016/j.fpsl.2020.100462)

4. G. El-Fawal, *J. Food Sci. Technol.* **51** (2014) 2234 (https://doi.org/10.1007/s13197-013-1255-9)
5. A. Nesic, J. Ruzic, M. Gordic, S. Ostojic, D. Micic, A. Onjia, *Composites, B* **110** (2017) 56 (http://dx.doi.org/10.1016/j.compositesb.2016.11.016)
6. N. Tabassum, M. A. Khan, *Sci. Hortic.* **259** (2020) 108853 (https://doi.org/10.1016/j.scienta.2019.108853)
7. H. Somashekarappa, Y. Prakash, K. Hemalatha, T. Demappa, R. Somashekar, *Indian J. Mater. Sci.* **2013** (2013) 307514 (http://dx.doi.org/10.1155/2013/307514)
8. X. Zhang, H. Guo, W. Luo, G. Chen, N. Xiao, G. Xiao, C. Liu, *Front. Bioeng. Biotechnol.* **10** (2022) 01 (https://doi.org/10.3389/fbioe.2022.989893)
9. E. Di Giuseppe, in *Reference Module in Earth Systems and Environmental Sciences*, S. A. Elias, Ed., Elsevier, Amsterdam, 2018 (https://doi.org/10.1016/B978-0-12-409548-9.10909-1)
10. Z. Lu, J. Huang, S. E, J. Li, L. Si, C. Yao, F. Jia, M. Zhang, *Carbohydr. Polym.* **250** (2020) 116919 (https://doi.org/10.1016/j.carbpol.2020.116919)
11. N. Aqdas, M. Z. Khalid, T. Shazia, A. Waseem, S. Muhammad, Z. Mohammad, *Int. J. Biol. Macromol.* **15** (2020) 993 (https://doi.org/10.1016/j.ijbiomac.2019.10.254)
12. M. El Achaby, Y. Essamlali, N. El Miri, A. Snik, K. Abdelouahdi, A. Fihri, A. Solhy, *J. Appl. Polym. Sci.* **131** (2014) 41042 (https://doi.org/10.1002/app.41042)
13. X. Sui, Y. Chu, J. Zhang, H. Zhang, H. Wang, T. Liu, C. Han, *Adv. Polym. Technol.* **2020** (2020) 8859658 (https://doi.org/10.1155/2020/8859658)
14. C. S. Reddy, P. K. Babu, K. Sudhakar, M. N. Prabhakar, P. Sudhakar, S. V. Pratap, S. H. R. Prasad, V. N. E. Reddy, M. C. S. Subha, K. C. Rao, *Polym. Res. J.* **7** (2013) 253 (https://www.researchgate.net/profile/Palla-Kumara-Babu/publication/281743945_miscibility_studies_of_hydroxyethyl_cellulose_and_poly_ethylene_glycol_polymer_blends/links/55f7c01a08aeafc8ac0569a1/miscibility-studies-of-hydroxyethyl-cellulose-and-poly-ethylene-glycol-polymer-blends.pdf)
15. G. El Fawal, H. Hong, X. Song, J. Wu, M. Sun, L. Zhang, C. He, X. Mo, H. Wang, *Appl. Biochem. Biotechnol.* **191** (2020) 1624 (https://doi.org/10.1007/s12010-020-03282-1)
16. K. C. Rao, M. C. S. Subha, C. S. Reddy, P. K. Babu, K. Sudhakar, M. N. Prabhakar, Y. Maruthi, U. S. K. Rao, *Int. J. Basic Appl. Chem. Sci.* **3** (2013) 73 (https://www.cibtech.org/J-CHEMICAL-SCIENCES/PUBLICATIONS/2013/Vol%203%20No.%201/10-004...Chowdoji...Miscibility...Blends...73-83.pdf)
17. B. Anwar, B. Bundjali, Y. Sunarya, I. M. Arcana, *Fibers Polym.* **22** (2021) 1228 (https://doi.org/10.1007/s12221-021-0765-8)
18. M. F. Zaltariov, *Cellul. Chem. Technol.* **55** (2021) 981 (https://doi.org/10.35812/CelluloseChemTechnol.2021.55.84)
19. Y. H. Wen, C. H. Tsou, M. R. de Guzman, D. Huang, Y. Q. Yu, C. Gao, Z. H. Wang, *Polym. Bull.* **79** (2022) 3847 (https://doi.org/10.1007/s00289-021-03666-1)
20. D. A. Rusmawati, I. Yuliasih, T. C. Sunarti, *IOP Conference Series: Earth and Environmental Science,* Vol. 443, (2020) International Conference on Food and Bio-Industry 2019, 29-30 July 2019, Bandung, Indonesia (https://doi.org/10.1088/1755-1315/443/1/012054)
21. E. Karavas, E. Georgarakis, D. Bikiaris, *Int. J. Pharm.* **313** (2006) 189 (https://doi.org/10.1016/j.ijpharm.2006.01.015)

22. Y. Prakash, D. Mahadevaiah, H. Somashekarappa, T. Demappa, R. Somashekar, *J. Res. Updates Polym. Sci.* **1** (2012) 24 (http://dx.doi.org/10.6000/1929-5995.2012.01.01.4)
23. R. Kumar, I. Mishra, G. Kumar, *J. Polym. Environ.* **29** (2021) 3770 (https://doi.org/10.1007/s10924-021-02143-0)
24. S. Patil, A. K. Bharimalla, A. Mahapatra, J. Dhakane-Lad, A. Arputharaj, M. Kumar, A. S. M. Raja, N. Kambli, *Food Biosci.* **44** (2021) 101352 (https://doi.org/10.1016/j.fbio.2021.101352)
25. A. Gleadall, in *Modelling Degradation of Bioresorbable Polymeric Medical Devices*, J. Pan, Ed., Elsevier Ltd., Amsterdam, 2015, p. 163 (https://doi.org/10.1533/9781782420255.2.163)
26. C. Ding, M. Zhang, G. Li, *Carbohydr. Polym.* **119** (2015) 194 (http://dx.doi.org/10.1016/j.carbpol.2014.11.057)
27. M. Voronova, N. Rubleva, N. Kochkina, A. Afineevskii, A. Zakharov, O. Surov, *Nanomaterials* **8** (2018) 1011 (https://doi.org/10.3390/nano8121011)
28. S. Wang, J. Ren, W. Li, R. Sun, S. Liu, *Carbohydr. Polym.* **103** (2014) 94 (http://dx.doi.org/10.1016/j.carbpol.2013.12.030)
29. J. F. Mukerabigwi, S. Lei, L. Fan, H. Wang, S. Luo, X. Ma, J. Qin, X. Huang, Y. Cao, *RSC Adv*. **6** (2016) 31607 (https://doi.org/10.1039/C6RA01759B)
30. M. Fiayaz, K. M. Zia, M. A. Javaid, S. Rehman, S. A. S. Chatha, M. Zuber, *Korean J. Chem. Eng*. **37** (2020) 2351 (https://doi.org/10.1007/s11814-020-0664-5)
31. A. D. French, M. S. Cintron, *Cellulose* **20** (2013) 583 (https://doi.org/10.1007/s10570-010-9420-z)
32. A. Emblem, in *Packaging Technology: Fundamentals, Materials and Processes*, A. Emblem, H. Emblem, Eds., Elsevier Ltd., Amsterdam, 2012, p. 287 (https://doi.org/10.1533/9780857095701.2.287)
33. S. Guzman-Puyol, J. J. Benítez, J. A. Heredia-Guerrero, *Food Res. Int.* **161** (2022) 111792 (https://doi.org/10.1016/j.foodres.2022.111792)
34. A. Aydogdu, E. Yildiz, Z. Ayhan, Y. Aydogdu, G. Sumnu, S. Sahin, *Eur. Polym. J.* **112** (2019) 477 (https://doi.org/10.1016/j.eurpolymj.2019.01.006)
35. R. Kumar, B. Rai, G. A. Kumar, *J. Polym. Environ.* **27** (2019) 2963 (https://doi.org/10.1007/s10924-019-01588-8)
36. T. Huhtamäki, X. Tian, J. T. Korhonen, R. H. Ras, *Nat. Protoc.* **13** (2018) 1521 (https://doi.org/10.1038/s41596-018-0003-z)
37. R. Poonguzhali, S. K. Basha, V. S. Kumari, *Polym. Bull.* **74** (2017) 2185 (https://doi.org/10.1007/s00289-016-1831-z)
38. P. Lu, H. Xiao, W. Zhang, G. Gong, *Carbohydr. Polym.* **111** (2014) 524 (https://doi.org/10.1016/j.carbpol.2014.04.071)
39. H. Y. Wu, T. X. Liu, C. H. Hsu, Y. S. Cho, Z. J. Xu, S. C. Liao, S. Y. Lien, *Materials* **10** (2017) 821 (https://doi.org/10.3390/ma10070821)
40. A. Zheng, Y. Xue, D. Wei, S. Li, H. Xiao, Y. Guan, *Soft Mater.* **12** (2014) 179 (https://doi.org/10.1080/1539445X.2013.831357)
41. T. T. Kararli, J. B. Hurlbut, T. E. Needham, *J. Pharm. Sci.* **79** (1990) 845 (https://doi.org/10.1002/jps.2600790922)
42. F. H. Zulkifli, F. S. J. Hussain, W. S. W. Harun, M. M. Yusoff, *Int. J. Biol. Macromol.* **122** (2019) 562 (https://doi.org/10.1016/j.ijbiomac.2018.10.156)

43. K. Beyaz, C. Vaca-Garcia, E. Vedrenne, N. Haddadine, A. Benaboura, S Thiebaud-Roux, *Int. J. Polym. Anal. Charact.* **24** (2019) 245 (https://doi.org/10.1080/1023666X.2019.1567085)
44. T. M. M. Swamy, B. Ramaraj, Siddaramaiah, *J. Appl. Polym. Sci.* **112** (2009) 2235 (https://doi.org/10.1002/app.29738)
45. J. B. Yin, K. Luo, X. S. Chen, V. V. Khutoryanskiy, *Carbohydr. Polym.* **63** (2006) 238 (https://doi.org/10.1016/j.carbpol.2005.08.041)
46. V. Mutalik, L. S. Manjeshwar, A. Wali, M. Sairam, B. Sreedhar, K. V. S. N. Raju, T. M. Aminabhavi, *J. Appl. Polym. Sci.* **106** (2007) 765 (https://doi.org/10.1002/app.25427).